Tuning response range of a transmission-based fiber-optic refractometer through LP_{11} mode

Guigen Liu,[1] Kaiwei Li,[1,2] Fang Dai,[1,2] Peng Hao,[1] Wenchao Zhou,[1,2] Yihui Wu,[1,*] and Ming Xuan[1]

[1]*State Key Laboratory of Applied Optics, Changchun Institute of Optics, Fine Mechanics and Physics, Chinese Academy of Sciences, Changchun 130033, China*

[2]*Graduate School of Chinese Academy of Sciences, Beijing 100039, China*

**Corresponding author: yihuiwu@ciomp.ac.cn*

Received January 16, 2014; revised February 27, 2014; accepted February 27, 2014; posted February 27, 2014 (Doc. ID 204900); published March 25, 2014

A kind of sensing scheme is theoretically proposed to efficiently tune the response range of a fiber-optic refractometer based on the adiabatic transmission of the higher-order LP_{11} mode. Near the cut-off condition, transmission of the LP_{11} mode is a strong function of the refractive index (RI) under detection; thus high sensitivity is achieved. The cut-off RI value is dependent on the waist diameter; therefore the response RI range with high sensitivity can be changed just by altering the waist diameter. Theoretical calculations reveal that the response range is effectively tuned from 1.43–1.438 to 1.35–1.365 when the waist diameter is reduced from 2.5 to 1 μm. The proposed fiber-optic sensor is also superior when used as an absorbing sensor since the higher-order mode LP_{11} has a much larger power fraction in the evanescent field compared with the fundamental mode LP_{01} of the same fiber.

OCIS codes: (060.2310) Fiber optics; (060.2370) Fiber optics sensors.
http://dx.doi.org/10.1364/OL.39.001961

Comprehensive investigations have been made on optical-fiber refractive index (RI) sensors, whose configurations have evolved from a simple form of tapered fiber [1] to a variety of new ones, including photonic crystal fiber [2], fiber Bragg grating [3], splicing of different fibers [4–6], bent fiber [7], etc. These fiber-optic RI sensors may be based on either transmission or wavelength shift, and many of them have researched a competitively high sensitivity. It is not difficult to observe that one common feature of these fiber-optic refractometers is that the highest sensitivity is always obtained at high RI approaching that of the fiber (~1.46 for silica fibers). It can be intuitively understood that the interaction between waveguide mode(s) and external RI is strongest when the external RI is close to that of the fiber because of the largest evanescent field. Despite the impressive sensitivity at high RI, their limitations are insurmountable in cases when low RIs need to be determined, e.g., the RI of biomolecule solution is near that of water (~1.333). Therefore it's of great interest to develop a refractometer with the highest sensitivity over a tunable response range, especially a low RI range.

Several reports may provide a way to deal with the above issue. One straightforward method may be that the response range can be tuned by changing the sensor's parameters. This is exemplified by [8,9], the lowest detectable RI is decreased by reducing the waist diameter of a tapered multimode fiber, but it is with the cost of reduction in the overall sensitivity over the whole RI range, and the sensitivity at low RI is still unsatisfying. As another potential technique, optical nanofibers featuring a large evanescent field can be used as high-sensitivity refractometers [10,11]. Unfortunately, the nanofiber-based refractometers are still not as sensitive at low RI as expected. The main reason may be that the fundamental mode LP_{01} transmitted in the nanofiber doesn't have a cut-off frequency, which suggests it's impossible to alter the fact that the largest evanescent field and thus highest sensitivity occur at high RI close to that of fiber, although the diameter is shrunk to a sub-wavelength scale. In one previous work of our group [12], we added a coating of silica nanospheres to the surface of a tapered fiber; this kind of refractometer combined the scattering effect of nanospheres and mode propagation of the tapered fiber; thus higher sensitivity and a wider detection range were achieved. Yet this nanoparticle modified fiber has lower sensitivity at low RI than at high RI, and it's practically difficult to control the nanosphere coating.

In this Letter, a novel RI sensing principle is theoretically proposed to conveniently tune the sensitive range by using the transmission of the higher-order mode of the LP_{11} through a tapered fiber. It takes advantage of the nonzero cut-off condition of the LP_{11} mode at the waist section, which makes the transmission decrease from ~1 to 0 within a narrow increment of ~0.01 in external RI near the cutoff. When the waist diameter reduces, the external RI corresponding to the cut-off condition of the LP_{11} mode is reduced; thus the response range is tuned to a lower RI range accordingly.

The proposed sensing scheme is illustrated in Fig. 1. The input modal field of LP_{11} is selectively excited as the launch field. It's practically feasible to selectively excite the LP_{11} mode with a high efficiency via the appropriate selection of launch field with intensity distribution and phase matching the mode field of LP_{11} [13,14]. Due to the rule of mode coupling [15], only LP_{1n} ($n = 1, 2, 3, \ldots$) modes can be possibly excited throughout the tapered fiber by the input LP_{11} mode. When the waist diameter

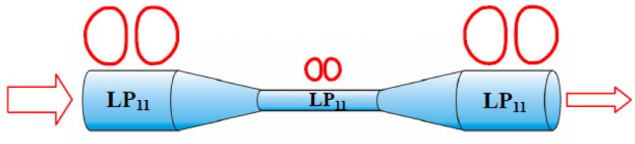

Fig. 1. Schematic drawing of the proposed working principle of a tapered sensing fiber, which transmits the LP_{11} mode.

is well chosen, the propagation of single LP_{11} mode can be achieved in the waist section with other higher-order modes being cut off. It would be ideal if the transition region is adiabatic and no mode coupling occurs; in this case, all power in the original LP_{11} mode is perfectly preserved until external RI approaches the cut-off value. Within the narrow RI range near the cut off of LP_{11}, the transmission dramatically decreases as RI increases, indicating an extremely high sensitivity.

In order to accurately calculate light propagation through the tapered fiber, a reliable simulation scheme of beam propagation method has been used. The technique to fabricate tapered fibers through chemical etching has been well established within our group [16,17]. Therefore, an etched tapered optical fiber is chosen as the model in this Letter, as schematically shown in Fig. 2(a). The transition length is set to be long enough to guarantee adiabatic transmission. In our simulations, core and cladding RIs are 1.449 and 1.445, respectively; the original core diameter is 8.2, wavelength is 633 nm, both translation regions are 5 mm long with an exponential shape as the case of a heat-drawn taper [18], and waist length is 3 mm.

Figure 2(b) plots the transmission versus external RI for a tapered fiber with a waist diameter of 1.3 μm. As external RI increases, the transmission remains almost unchanged at the first stage (RI < 1.387), then decreases swiftly over a narrow RI range of 1.387–1.405 (second stage), and at last is reduced to zero in excess of 1.405 (third stage). The left column of insets in Fig. 2(b) manifest field evolution along the tapered fiber at three different external RI values. In the first stage, the initial power is well preserved and squeezed in the tiny waist, which is typically shown by the inset of field evolution in the meridian plane at RI of 1.36. In the second stage, the field greatly expands into the external medium, and some power is lost, as typically visualized by the meridian inset at RI of 1.396. In the third stage, no transmitted power is seen; a typical field map of this case is clearly shown by the meridian inset at RI of 1.43. The input LP_{11} mode field has a lobe shape over the cross section as shown by the upper-right inset in Fig. 2(b); the lobe shape is well conserved until the waist section if the LP_{11} mode is not cut off within the waist, which is in accordance with the aforementioned rule of mode coupling. The column of mid-waist field maps in Fig. 2(b) typically show the transverse distribution of the LP_{11} modal field when it is far below (first stage), near (second stage), and well beyond (third stage) cutoff. The transmission drops swiftly as external RI increases at the second stage, which is the only response range with high sensitivity. It is noteworthy that the transmission maintains close to unit at the first stage, suggesting that it facilitates to obtain a high signal-to-noise ratio (SNR). As a comparison to the results of previous transmission-based tapered optical-fiber refractometers [8,9], our refractometer is much more sensitive since a larger variation in transmission occurs within a much narrower RI variation (in our case, transmission is reduced from 1 to 0 when RI increases from 1.387 to 1.405; in [8], transmission from 1 to ~0.2 when RI from 1.40 to 1.45).

Figure 2(c) shows the transmission versus external RI for five tapered fibers with different waist diameters.

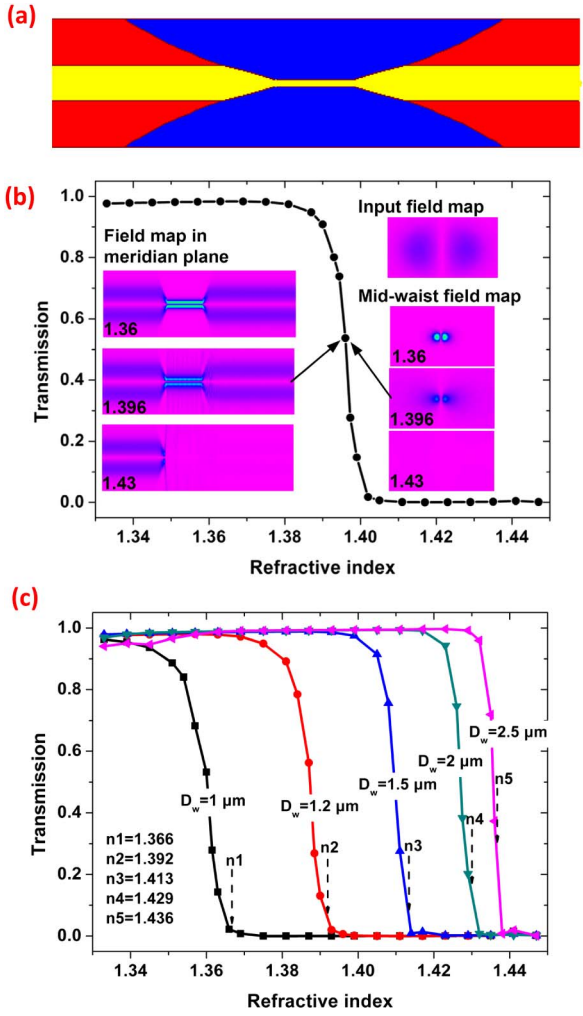

Fig. 2. (a) Schematic model of an etched tapered fiber. Yellow, core; red, cladding; blue, RI under detection. (b) Transmission with respect to external RI for a tapered fiber with a 1.3 μm thick waist. Left column of insets illustrate the field distribution within meridian plane under the denoted external RI. Right column of insets illustrate field distribution over the cross section at mid-waist point, except the top one showing the input field of LP_{11} mode. (c) Transmission versus external RI at different waist diameters. Dashed vertical arrows denote the RI values ($n1$–$n5$) corresponding to the cutoff of the LP_{11} mode at different waist diameters (denoted as D_w).

Clearly, the response RI range is conveniently tuned by changing its waist diameter. Specifically, the response range is tuned from 1.43–1.438 to 1.35–1.365 when the waist diameter is reduced from 2.5 to 1 μm. The underlying mechanism for this tunability lies in the alteration of the cut-off RI value of the LP_{11} mode caused by diameter change in the waist section, as indicated by the dashed arrows in Fig. 2(c), and accordingly the sensitive RI range is shifted. Note that the transmission is not immediately reduced to zero when the LP_{11} mode reaches cutoff, which may be ascribed to the transmission of slowly attenuated leaky mode just below cutoff in the waist section [19].

Now let's consider the reasons why other higher-order modes except LP_{11} are not chosen for the proposed sensing scheme. The potentially existing bound modes of a

fiber are determined by the V number, which is defined as

$$V = \frac{\pi D}{\lambda}\sqrt{n_{\mathrm{co}}^2 - n_{\mathrm{cl}}^2}, \tag{1}$$

where D, λ, n_{co}, and n_{cl} are fiber diameter, wavelength in vacuum, core RI, and cladding RI, respectively. The LP_{11} mode has a cut-off V number of 2.405, which is the lowest compared to other higher-order modes, e.g., the closest LP_{02} and LP_{21} modes, both of which have the same cut-off V number of 3.832. Under such condition that V is between 2.405 and 3.832, only one higher-order mode of LP_{11} (except the fundamental mode LP_{01}) is supported; thus a pure propagation is obtained without the possibility of coupling between higher-order modes, avoiding fluctuations in output power, which are adverse to transmission-based optical-fiber refractometers [20]. LP_{0n} $(n \geq 2)$ modes are inappropriate since they can get coupled to fundamental LP_{01} mode, which cannot be cut off (cut-off V number for LP_{01} mode is 0); if the transition is nonadiabatic, this coupling will also introduce fluctuation. As clearly shown in Fig. 3, other higher-order modes of LP_{m1} $(m \geq 2)$ have a large fraction of power residing in the core even when it's cut off, the detailed reasons for this can be found in [19]; however, the LP_{11} mode transmits virtually all the power via evanescent field when it's near cutoff. The strong evanescent field of the LP_{11} mode gives rise to extremely high sensitivity when it works near the cut-off condition, complying with the results in Figs. 2(b) and 2(c).

Because LP_{01} and LP_{11} modes cannot get coupled to each other throughout the tapered fiber, they propagate independently. Figure 4 illustrates the response of tapered fibers guiding both LP_{01} and LP_{11} modes to measurand RI. Take tapered fiber 1 (namely, F1 in Fig. 4) whose waist diameter is 1.4 μm as an example, both LP_{01} and LP_{11} modes have the same initial normalized power of 0.5 (with a total power of 1). The output total power (F1, total), modal power in LP_{01} (F1, LP_{01}) and LP_{11} (F1, LP_{11}) modes as a function of external RI are shown in Fig. 4. Obviously, the total power is approximately the summation of LP_{01} and LP_{11} modal power when both modes exist over the RI range of 1.38–1.41 and is virtually equal to LP_{01} modal power when only the LP_{01} mode survives over the RI range of 1.41–1.45. The first response

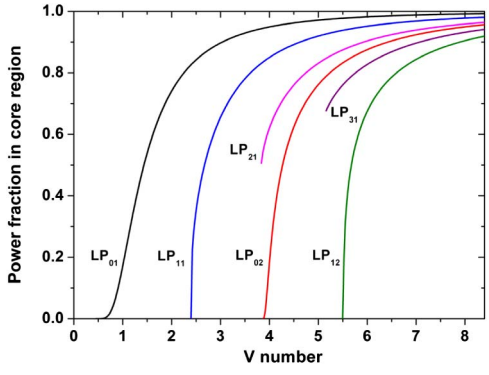

Fig. 3. Power fraction in the core region as a function of V number for the six lowest-order modes. Upon cutoff, LP_{21} and LP_{31} have a large power fraction in the core region.

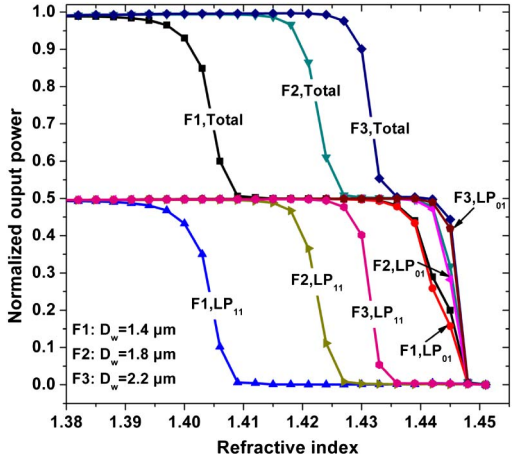

Fig. 4. Transmitted power of tapered fibers with different waist diameters (denoted by D_w) as a function of external RI. Fibers 1, 2, and 3, which are designated as F1, F2, and F3, have D_w of 1.4, 1.8, and 2.2 μm, respectively. The input field consists of two modes LP_{01} and LP_{11}, which have the equal initial power. For each fiber, total power, modal power of LP_{01}, and modal power of LP_{11} are monitored simultaneously.

range of 1.395–1.41 and the second response range of 1.433–1.448 in the total power curve (F1, total) are concerned, respectively, with the LP_{11} and LP_{01} mode, which is verified by the same response range in curves for LP_{11} (F1, LP_{11}) and LP_{01} (F1, LP_{01}) mode, respectively. The slightly higher total power over the LP_{01} mode when the LP_{11} mode is cut off within the second response range may be due to the existence of weak leaky modes as discussed for the nonzero transmission upon cutoff of the LP_{11} mode in Fig. 2(c). No fluctuation in the total power curve proves that the LP_{01} and LP_{11} modes cannot couple due to the cylindrical symmetry of the tapered fiber, verifying the former predictions of independent transmission of LP_{01} and LP_{11} modes. The first response range concerned with the LP_{11} mode is again effectively tuned by varying the waist diameter as shown by the results of F2 and F3 in Fig. 4. Note that the second response range (close to the fiber RI) concerned with the LP_{01} mode stays almost unchanged, which supports the conclusion that it's inefficient to tune the response range by the fundamental mode as mentioned in the introduction of this Letter. Through this comparison, the ability of the LP_{11} mode in the tuning response range clearly stands out. The independent transmission of the LP_{01} and LP_{11} modes is of great practical interest because it can relax the aforementioned demands on selective excitation of LP_{11} with strong suppression of other modes. For example, if the V number of the input fiber is between 2.405 and 3.832, one can fully excite all the possible bound modes of LP_{01} and LP_{11}, but only makes use of LP_{11} mode, in which case LP_{01} is regarded as a bias in transmission and can be subtracted. Apparently, the bias takes a portion of the dynamic range of the detector used for determining transmission, which will unavoidably bring the cost of reduction in SNR. Therefore, the most ideal case is still to only excite initial power in the LP_{11} mode without fields of other modes including LP_{01}.

For practical applications, the proposed sensing scheme based on the LP_{11} mode will be greatly suitable

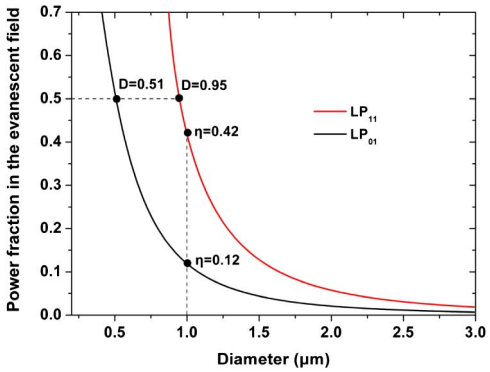

Fig. 5. Power fraction in the evanescent field (denoted by η) versus fiber diameter (denoted by D).

for situations where RI changes within a small range, e.g., the binding of biomolecules. Before application, one needs to select the appropriate waist diameter to make sure that the RI under detection is well within the response range. It's also of great interest to note the advantage of this higher-order-mode fiber used as an absorption sensor. Compared to the fundamental mode LP_{01} of the same fiber, the LP_{11} mode has a much larger power fraction in the evanescent field, which is well illustrated in Fig. 5. In the calculations, RIs of the fiber and external medium are assumed to be 1.449 and 1.333, respectively; the wavelength is 633 nm. On the one hand, for a 1 μm thick fiber immersed in water, the power fraction of 0.42 for the LP_{11} mode is more than three times higher than 0.12 for the LP_{01} mode. On the other hand, if half the power in the evanescent field is expected, one needs to shrink the fiber to be 0.51 μm thick for the LP_{01} mode, while a thickness of 0.95 μm is enough for the LP_{11} mode, which suggests a relaxation on the sensor fabrication. Because the transmission is greatly reduced when the sensor works near the cutoff of the LP_{11} mode, it inevitably introduces the risk of a lower SNR if one attempts to increase the sensitivity by making it work near the cutoff. Therefore, careful selection of the working point is also desired for the proposed sensor serving as an absorption probe.

In conclusion, a novel RI sensing scheme based on the transmission of the higher-order mode of LP_{11} through a tapered optical fiber has been proposed and theoretically studied. It not only exhibits high sensitivity, but also can effectively tune the response RI range by just simply changing the waist diameter. The proposed sensor is also attractive when it is used as an absorption probe because the higher-order mode LP_{11} has a much larger power fraction in the evanescent field than the fundamental mode LP_{01} of the same fiber.

This work was supported by the National Natural Science Foundation of China (nos. 61102023 and 11034007), the development plan project of Jilin Province Science and Technology (no. 20120329), and the National High Technology Research and Development Program of China (no. 2012AA040503).

References

1. J. Villatoro, D. Monzón-Hernández, and D. Talavera, Electron. Lett. **40**, 106 (2004).
2. B. Lee, S. Roh, and J. Park, Opt. Fiber Technol. **15**, 209 (2009).
3. W. Liang, Y. Huang, Y. Xu, R. K. Lee, and A. Yariv, Appl. Phys. Lett. **86**, 151122 (2005).
4. Q. Wu, Y. Semenova, B. Yan, Y. Ma, P. Wang, C. Yu, and G. Farrell, Opt. Lett. **36**, 2197 (2011).
5. M. Han, F. Guo, and Y. Lu, Opt. Lett. **35**, 399 (2010).
6. P. Wang, L. Bo, C. Guan, Y. Semenova, Q. Wu, G. Brambilla, and G. Farrell, Opt. Lett. **38**, 3795 (2013).
7. G. Liu, K. Li, P. Hao, W. Zhou, Y. Wu, and M. Xuan, Sens. Actuators A Phys. **201**, 352 (2013).
8. D. Monzón-Hernández, J. Villatoro, and D. Luna-Moreno, Sens. Actuators B Chem. **110**, 36 (2005).
9. S. Guo and S. Albin, Opt. Express **11**, 215 (2003).
10. P. Polynkin, A. Polynkin, N. Peyghambarian, and M. Mansuripur, Opt. Lett. **30**, 1273 (2005).
11. L. Zhang, P. Wang, Y. Xiao, H. Yu, and L. Tong, Lab Chip **11**, 3726 (2011).
12. G. Liu, Y. Wu, K. Li, P. Hao, P. Zhang, and M. Xuan, IEEE Photon. Technol. Lett. **24**, 658 (2012).
13. W. Q. Thornburg, B. J. Corrado, and X. D. Zhu, Opt. Lett. **19**, 454 (1994).
14. M. C. Frawley, A. Petcu-Colan, V. G. Truong, and S. N. Chormaic, Opt. Commun. **285**, 4648 (2012).
15. L. C. Bobb, P. M. Shankar, and H. D. Krumboltz, J. Lightwave Technol. **8**, 1084 (1990).
16. Y. Wu, X. Deng, F. Li, and X. Zhuang, Sens. Actuators B Chem. **122**, 127 (2007).
17. K. Li, G. Liu, Y. Wu, P. Hao, W. Zhou, and Z. Zhang, Talanta **120**, 419 (2014).
18. T. A. Birks and Y. W. Li, J. Lightwave Technol. **10**, 432 (1992).
19. A. W. Snyder and J. D. Love, *Optical Waveguide Theory* (Chapman & Hall, 1983), Chap. 24.
20. S. Lacroix, R. Bourbonnais, F. Gonthier, and J. Bures, Appl. Opt. **25**, 4421 (1986).